Enzyme and Microbial Technology 47 (2010) 372–376

Contents lists available at ScienceDirect

Enzyme and Microbial Technology

journal homepage: www.elsevier.com/locate/emt

Directed evolution of tyrosinase for enhanced monophenolase/diphenolase activity ratio

Vered Shuster Ben-Yosef, Mor Sendovski, Ayelet Fishman*

Department of Biotechnology and Food Engineering, Technion-Israel Institute of Technology, Haifa 32000, Israel

ARTICLE INFO

Article history:
Received 29 May 2010
Received in revised form 1 August 2010
Accepted 24 August 2010

Keywords:
Tyrosinase
Directed evolution
Selectivity
Catechol

ABSTRACT

Tyrosinases are copper-containing enzymes which perform two reactions, the hydroxylation of tyrosine to 3,4-dihydroxyphenylalanine (L-DOPA) and the subsequent oxidation to form dopaquinone. The latter diphenolase activity is much faster than the monophenolase activity, limiting the use of tyrosinases for diphenol synthesis. The key residues influencing tyrosinase specificity are not well known. Random mutagenesis was performed on tyrosinase from *Bacillus megaterium* in order to find variants with altered selectivity. A high throughput colorimetric screening assay in 96-well plates was used to evaluate separately the monophenolase and diphenolase activity. Variant R209H exhibited a 1.7-fold increase in monophenolase activity accompanied by a 1.5-fold decrease in diphenolase activity, resulting in a 2.6-fold improvement in the monophenolase/diphenolase activity ratio. *In silco* modeling suggested that the imidazole group of the histidine residue obstructs the entrance to the active site thus interfering with L-DOPA binding to CuB. This work highlights a new amino acid residue that is important for catalysis of monophenols and supports the hypothesis that tyrosine and L-DOPA bind differently in the active site.

1. Introduction

Tyrosinases (EC 1.14.18.1) are copper-containing enzymes which are widely distributed throughout the phylogenetic scale, from bacteria to humans [25]. Molecular oxygen is used by tyrosinases to catalyze two successive enzymatic reactions: (i) the *ortho*-hydroxylation of monophenols to *ortho*-diphenols (monophenolase activity) and (ii) the oxidation of *ortho*-diphenols to *ortho*-quinones (diphenolase activity). The resulting highly reactive *ortho*-quinones auto-polymerize to melanin [12,23]. Tyrosinases belong to the type 3 copper-containing protein family together with catechol oxidase, that exhibits only diphenolase activity, and the oxygen-carrier hemocynanine [6,19]. Although these enzymes share similar active sites of two coupled copper ions, CuA and CuB which are coordinated by six histidine residues, their physiological activities are different [7,28]. Presently, there is an increasing interest in using tyrosinases in industrial applications such as wastewater treatment, bioremediation, and phenol detection using enzymatic biosensors [12,25].

The ability of tyrosinases to convert monophenols into diphenols has stimulated studies regarding the production of various *ortho*-diphenols (also referred to as substituted catechols). Catechols are important intermediates for the synthesis of pharmaceuticals, agrochemicals, flavors, polymerization inhibitors, and antioxidants [12,15,18,29]. It should be noted that manufacture of these substituted dihydroxylated compounds by chemical routes is difficult due to the employment of aggressive reagents, expensive and complicated starting materials, multiple reaction steps, and low yields [13,14].

Despite the great potential, the use of tyrosinases for catechol synthesis has been limited since their diphenolase activity is much faster than the monophenolase activity [14]. There are only few reports in the literature on utilization of tyrosinase for production of catechols, such as hydroxytyrosol and 3,4-dihydroxyphenylalanine (L-DOPA) from tyrosol and tyrosine, respectively, under reducing conditions [9,11,16,18]. In Nature, there is one reported unique tyrosinase from *Ralstonia solanacearum* with an abnormally high tyrosine hydroxylation/DOPA oxidase ratio [14].

There is a vast amount of literature available on the mechanism and biochemical nature of tyrosinases including one crystal structure of *Sterptomyces castaneoglobisporus* tyrosinase [5,10,17], however, the information on the catalytic residues involved in catalysis is yet limited [20,24]. In the present research, we employed directed evolution on tyrosinase from *Bacillus megaterium* that was previously isolated and characterized in our lab, in an attempt to improve its monophenolase/diphenolase activity ratio. Directed evolution is nowadays a recognized tool in biocatalysis that mimics the Darwinian concept of mutation and selection, in order to get a variant with the desired properties [22,30]. This work describes the discovery of one variant, R209H, with a 2.6-fold improvement in the monophenolase/diphenolase activity ratio.

* Corresponding author. Tel.: +972 4 829 5898; fax: +972 4 829 3399.
E-mail address: afishman@tx.technion.ac.il (A. Fishman).

0141-0229/$ – see front matter © 2010 Elsevier Inc. All rights reserved.
doi:10.1016/j.enzmictec.2010.08.008

Table 1
Primers used in this study.

Primer name	Sequence[a] 5′ → 3′	Restriction enzyme
NcoI Front[b,c]	GAGGTTAAACCATGGGTAACAAGTATAGAGTTAGAAAAAACG	*Nco*I
BglII Reverse[c]	CTGCTGTTTCTAGATCTGGTTATGAGGAACGTTTTGATTTTC	*Bgl*II
BglII his Reverse	CTGCTGTTTCTAGATCTGGTTAATGGTGGTGATGGTGATGTGAGG AACGTTTTGATTTTC	*Bgl*II
R209H His-arg Forward[c]	CCACAGCTTCACAATCGCGTACACCGTTGGGTTGGC	
R209H His-arg Rear[c]	CATCTGTCCGCCAACCCAACGGTGTACGCGATTG	

[a] The restriction sites are underlined.
[b] Primer NcoI Front generates an NcoI restriction site within the *tyr* gene by changing the second codon AGT to GGT, creating a serine to glycine change in the translated product of the modified *tyr* gene.
[c] These primers were used to generate the wild-type from the mutant (histidine to arginine replacement). The specific codons are marked by a shaded background.

Currently, there are no reports on directed evolution of tyrosinases for any purpose, and this novel variant provides new insight to an important residue influencing the monophenolase activity.

2. Materials and methods

2.1. Chemicals

L-DOPA was purchased from Acros (Geel, Belgium) and L-tyrosine disodium salt was purchased from Sigma–Aldrich (Rehovot, Israel).

2.2. Bacterial strains and culture conditions

B. megaterium was isolated from soil and stored at −80 °C, as described by Shuster et al. [26]. *Escherichia coli* BL21 (DE3; Novagen, Darmstadt, Germany) was used as the host for plasmid pET9d/tyr containing the tyrosinase gene [26]. *E. coli* transformants were grown in a Luria–Bertani medium containing 0.025 mg ml^{-1} kanamycin at 37 °C for 12 h.

2.3. Random mutagenesis of tyrosinase

The oligonucleotides used in this study are presented in Table 1. Plasmid DNA was extracted from *E. coli* BL21(DE3) using a Midi Kit (Promega, WI, USA) or a Mini Kit (Qiagen, CA, USA) and served as a template to amplify the *tyr* gene using error-prone PCR (epPCR) with 30 pmol of each primer (NcoI Front and BglII Reverse, Table 1) as described in Brouk et al. [4]. The PCR product was cloned as described previously [26] and single colonies were picked into 96-well plates containing LB with 0.025 mg ml^{-1} kanamycin and 25% glycerol, and were stored in −80 °C. These plates served as master plates for further work.

2.4. Screening for improved or altered activity

A high throughput assay for enhanced activity on L-tyrosine or L-DOPA was developed based on the method described by Bottcher and Bornscheuer for esterase activity with some modifications [2]. Screening for mutants with improved activity was performed by picking colonies from glycerol stocks stored in 96-well plates using a library copier VP 381 (V&P scientific, Inc., San Diego, CA, USA) and transferring into 96 deep well plates with a plastic lid (ABgene, Thermo Fisher Scientific, Epson, United Kingdom) containing 1.2 ml of LB with 0.025 mg ml^{-1} kanamycin. The cells were grown for 18 h at 37 °C with shaking at 250 rpm in an incubator shaker (TU-400 Orbital Shaker Incubator, MRC, Holon, Israel), followed by centrifugation at 2000 × *g* for 15 min, at 4 °C using a Sigma-4K15 centrifuge (Sigma, Osterode, Germany). The cell pellets were re-suspended in 300 μl of 50 mM sodium phosphate buffer, pH 8, from which 100 μl were removed to measure the cell density (OD at 600 nm, approximately 1.2). A second centrifugation step (2000 × *g*, 15 min, at 4 °C) was carried out and the cell pellets were broken by re-suspension in 300 μl lysis buffer (50 mM sodium phosphate buffer pH 8, 300 mM NaCl, 0.1% lysozyme and 1 unit ml^{-1} DNase1). The suspended cells were incubated for 30 min at 4 °C followed by freezing at −80 °C for 1 h and then thawing them at 37 °C for approximately 2 h with gentle shaking. The thawed cells were centrifuged at 3000 × *g* for 25 min, at 16 °C, and 20 μl supernatant were taken for the activity test with 1 mM L-tyrosine or L-DOPA at pH 7.0. The formation of L-dopachrome was measured periodically at 475 nm for both substrates (OPTImax tunable microplate reader, Molecular Devices, Sunnyvale, CA, USA) following a 25 min incubation period at 28 °C. The best variants were sequenced using the dideoxy chain termination technique (Multidisciplinary Laboratories, Technion, Haifa, Israel). The universal primers of T7 promotor and terminator were used for sequencing. Vector NTI (Invitrogen, CA, USA) was used for analyzing the sequencing results.

2.5. Validation of the screening assay

The transformants were grown in 25 ml TB medium (tryptone 1.2%, yeast extract 2.4%, glycerol 0.4% and phosphate buffer 89 mM) with 0.025 mg ml^{-1} kanamycin for 18 h and the cells were harvested by centrifugation (8000 × *g*, 10 min, 25 °C) and re-suspended with 10 ml 50 mM phosphate buffer pH 7.0. The suspended cells were broken by sonication (VibraCell VCX750 with a CV33 transducer and an SM0401 tip, Sonics & Materials Inc., Newtown, CT) by a 5 min treatment at a relative output power of 0.4 with 0.5 duty periods [27]. The broth was centrifuged for 20 min at 2000 × *g* at 15 °C and the supernatant was used as a crude cellular extract for enzymatic activity determination.

2.6. Reversion of the R209H mutation back to WT

The generation of the wild-type from the R209H variant was carried out using overlap extension PCR as described in Brouk et al [3]. Shortly, two pairs of primers were designed to create the back replacement of histidine to arginine (Table 1). The first PCR fragment was amplified using primers NcoI Front and R209H His-arg Rear, while the second was amplified using primers R209H His-arg Forward and BglII Reverse using the PCR program that was described previously [26] with an annealing temperature of 55 °C rather than 52 °C. The two fragments were combined during the final reassembly PCR in 1:1 molar ratio using the outer primers NcoI Front and BglII Reverse with the same PCR program. The assembled PCR fragment was cloned as describe previously [26]. The new generated wild-type (H209R) was grown in 25 ml TB medium and the cells were broken by sonication and centrifuged as described above. The enzymatic activities of R209H and H209R were measured using a crude cellular extract with 2 mM L-tyrosine or L-DOPA as substrates for monophenolase and diphenolase activity, respectively.

2.7. Purification of active His_6-tag tyrosinase

A His_6-tag was coupled to the C-terminal of the mutant tyrosinase gene using high fidelity Phusion DNA polymerase (New England Biolabs, MA, USA) and NcoI Front and BglII his Reverse primers (Table 1), followed by transformation to *E. coli* BL21(DE3). The His_6-tagged tyrosinase was purified in one step using a Ni(II)-bound affinity column (HisTrap HP; Ameshram Biosciences, Giles, UK) as described earlier [26] with slight changes in the binding, elution and dialysis buffers. The binding buffer contained 20 mM Tris–HCl buffer, pH 7.5, 500 mM NaCl, and 20 mM imidazole while the elution buffer contained 20 mM Tris–HCl buffer, pH 7.5, 500 mM NaCl and 500 mM imidazole. The fractions containing tyrosinase were collected and dialyzed against 50 mM Tris–HCl buffer pH 7.0 at 4 °C.

2.8. Characterization of R209H tyrosinase

The values of K_m and V_{max} for the purified His_6-tag R209H tyrosinase and the His_6-tag wild-type enzyme (Table 2) were determined by a colorimetric assay with the following conditions: 200 μl 50 mM Tris–HCl buffer pH 7.0, 0.01 mM $CuSO_4$, 28 °C, employing 3 μg ml^{-1} of purified enzyme, and substrate concentrations ranging from 0.1 to 6.0 mM for L-DOPA and D-DOPA, and 0.02 to 6.0 mM for L-tyrosine. The formation of L-dopachrome (ε = 3600 M^{-1} cm^{-1}) was monitored by measuring the absorbance at 475 nm. Specific activity was calculated as the ratio of the conversion rate and the total protein content as determined by the Bradford analysis method, with bovine serum albumin as a calibration standard (Bio-Rad Protein Assay Kit). All measurements were performed in triplicates in 96-well plates and the light path was determined as 0.68 cm. In addition, the hydroxylation of L-tyrosine was determined by measuring the decrease in tyrosine concentration using high performance liquid chromatography (HPLC) as described earlier [26]. 2 mM L-tyrosine was added to 5 ml reaction volume containing 50 mM Tris–HCl at pH 7.0, 0.01 mM $CuSO_4$ and 5.4 μg ml^{-1} of purified enzyme at 28 °C for 15 min. The reaction was stopped periodically by adding 0.5 ml of the reaction mixture to 0.1 ml 2 M HCl. The samples were filtered using PVDF 0.45 μm filters (Millex HV, Millipore, Cork, Ireland) and analyzed. A calibration curve was made with a commercial standard at 275 nm wavelength.

2.9. Homology models of wild-type tyrosinase and variant R209H

A homology model of wild-type tyrosinase from *B. megaterium* was prepared using the alignment mode in the SWISS-MODEL workspace [1]. Residues Gly33 through Asn247 were aligned and modeled based on the crystal structure of *Streptomyces castaneoglobisporus* tyrosinase (1WX2, [17]). The model of variant R209H

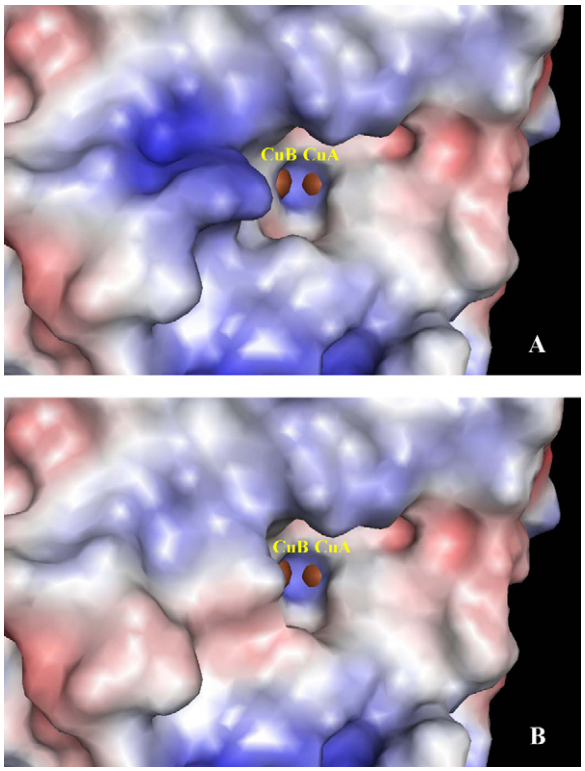

Fig. 1. Calculated surface electrostatic potential of the active site entrance of wild-type tyrosinase (A) and variant R209H (B). Structure was prepared based on the crystal structure of *Streptomyces castaneoglobisporus* tyrosinase (1WX2, [17]). Surface potentials were calculated using the *in vacuo* approximation of Pymol (http://www.pymol.org). The distribution of patches of positive or negative potentials are shown in *blue* and *red*, respectively. The copper atoms are colored in orange.

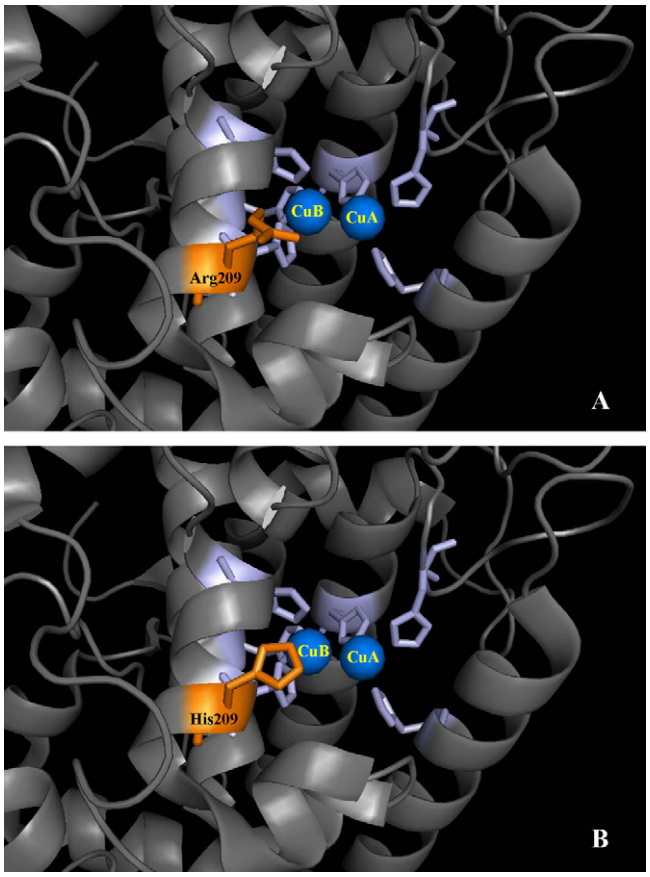

Fig. 2. Tyrosinase active site entrance in wild-type tyrosinase (A) and variant R209H (B). The structure was prepared based on the crystal structure of *Streptomyces castaneoglobisporus* tyrosinase (1WX2, [17]). Molecular graphics were performed using Pymol (http://www.pymol.org). The copper atoms (blue) are coordinated by six histidine residues (purple). The mutated residue H209 (orange) obstructs the access to the CuB atom.

was prepared by introduction of a point mutation to the wild-type using PYMOL mutagenesis wizard (http://www.pymol.org). Figs. 1 and 2 were prepared using PYMOL.

3. Results and discussion

3.1. Screening for improved or altered activity

A high throughput assay for enhanced activity on L-tyrosine or L-DOPA was developed. The aim was to locate mutants that have higher activity on L-tyrosine and lower activity on L-DOPA. The assay is composed of a growth stage in which the mutants are grown in deep 96-well polypropylene plates followed by cell breakage using a lysis buffer, and subsequent biotransformation by contacting the cell extract with 1 mM L-tyrosine or L-DOPA at pH 7.0. Nearly 2000 colonies were screened and 8 variants were found to possess higher activity on L-tyrosine compared with wild-type. Each variant contained one or two amino acid replacements.

The best variants from the 96-well plates were grown on larger scale (25 ml) as described in material and methods section, in order to confirm the modified activity. Biotransformations were carried out using 1 mM L-tyrosine or L-DOPA as substrates for monophenolase and diphenolase activity, respectively, and the enzyme activity was examined as described earlier [26]. The cell extract from variant R209H, exhibited a 1.8-fold increase in activity on L-tyrosine as a substrate accompanied by a 1.6-fold decrease in activity on L-DOPA suggesting an enhanced monophenolase/diphenolase activity ratio relative to the wild-type. In order to validate the contribution of the R209H substitution to the modified activity, a back replacement was performed to obtain H209R and the biotransformations were carried out using L-tyrosine or L-DOPA. Upon reversion of histidine to arginine, the modified activity diminished, and the monophenolase/diphenolase activity ratio (V_{max} tyr/V_{max} L-DOPA) was identical to the original wild-type activity (0.09 for both enzymes, the wild-type and the new variant H209R).

Table 2
Kinetic constants of wild-type tyrosinase and variant R209H.

	Substrate	K_m (mM)	V_{max} (μmol min^{-1} mg^{-1})	k_{cat} (s^{-1})	k_{cat}/K_m (s^{-1} mM^{-1})	V_{max} tyr/V_{max} L-DOPA
wt	L-Tyrosine	0.038 ± 0.005	2.2 ± 0.05	1.29	34.05	0.12
	L-DOPA	0.40 ± 0.04	18.0 ± 0.51	10.59	26.47	
	D-DOPA	1.20 ± 0.14	10.8 ± 0.49	6.35	5.29	
R209H	L-Tyrosine	1.3 ± 0.24	3.8 ± 0.24	2.24	1.72	0.31
	L-DOPA	0.62 ± 0.04	12.2 ± 0.25	7.18	11.58	
	D-DOPA	3.8 ± 0.27	11.7 ± 0.45	6.88	1.81	

Organism	Accession no.	CuB binding site
B.megaterium-wt	ACC86108	204 HNRVH**R**WVGGQMGVVPTAPNDPVFFLHH 231
B.megaterium-R209H		204 HNRVH**H**WVGGQMGVVPTAPNDPVFFLHH 231
R.solanacearum	NP_518458	227 HNTVH**N**NIGAFMPTA-ASPRDPVFMMHH 253
S.castaneoglobisporus	AAP33665	190 HNRVH**V**WVGGQMATG-VSPNDPVFWLHH 216
M.musculus	NP_035791	363 HNALH**I**FMNGTMSQVQGSANDPIFLLHH 390
		** :* :.. * :..**:* :**

Fig. 3. Amino acid sequence alignment at the CuB region of tyrosinase from *B. megaterium*-wt, *B. megaterium*-R209H, *R. solanacearum* NP_518458, *S. castaneoglobisporus* and *M. musculus*. Conserved histidine residues directly involved in copper binding are marked in the shaded background. Asterisks (*) denote conserved residues in all sequences. The amino acids at position 209 are shown in bold. Alignment was generated using CLUSTAL-W software (http://www.ebi.ac.uk/clustalw).

3.2. Characterization of the R209H variant

In order to further characterize variant R209H, a His_6-tag was coupled to the C-terminal of the mutant gene. The His_6-tagged R209H tyrosinase was purified using a Ni(II)-bound affinity column and the kinetic parameters for the mutant and wild-type enzymes were determined for L-DOPA, L-tyrosine and D-DOPA (Table 2). Variant R209H exhibited a 1.7-fold increase in k_{cat} for monophenolase activity accompanied by a 1.5-fold decrease in k_{cat} of the diphenolase activity relative to the wild-type (Table 2). Although the diphenolase activity of R209H is still higher than its monophenolase activity (12.2 μmol min^{-1} mg^{-1} vs. 3.8 μmol min^{-1} mg^{-1}, respectively), its monophenolase/diphenolase activity ratio is 2.6-fold higher than the wild-type ratio (0.31 vs. 0.12, respectively). Furthermore, a 1.6-fold increase in the monophenolase activity of variant R209H vs. the wild-type was also shown using HPLC analysis by monitoring directly the decrease in L-tyrosine during the reaction (data not shown). This examination confirmed the enhanced monophenolase activity of variant R209H determined colorimetrically by following dopachrome formation.

In order to investigate the reason for the change in selectivity of variant R209H, *in silico* homology modeling was used. A three-dimensional structure of the *B. megaterium* tyrosinase was created using the SWISS-MODEL workspace based on the known crystal structure of tyrosinase from *S. castaneoglobisporus* (Figs. 1 and 2). The observed differences in activity ratio seem to stem from different structural requirements of monophenolase and diphenolase activities as reported earlier [20,21,24]. It is suggested that the imidazole group of the His residue obstructs the entrance to the active site thus interfering with L-DOPA binding to CuB (Fig. 1). At the same time, the access of L-tyrosine to the CuA site is easier, as demonstrated from the higher k_{cat} value of the mutant. Olivares et al. mutated residue Q378 (analogous to P219 in tyrosinase from *B. megaterium*) located near the CuB binding site of mouse tyrosinase [20] (Fig. 3). Variant Q378H obtained through site-directed mutagenesis had a monophenolase/diphenolase activity ratio of 1.9-fold greater than wild-type, although the activity rate for L-DOPA was higher for both mutant and wild-type, similarly to *B. megaterium* tyrosinase and variant R209H. The K_m of Q378H for L-tyrosine remained constant while the affinity for L-DOPA was 50-fold lower resulting in higher affinity for tyrosine. In contrast, variant R209H of *B. megaterium* tyrosinase showed similar affinity for L-DOPA and a 34-fold increase in K_m for L-tyrosine resulting in lower affinity for tyrosine, suggesting that the main effects of the mutation are through substrate/product efflux rather than binding affinity. Furthermore, while the Q378H mutant of mouse tyrosinase exhibited an increase in the catalytic efficiency for tyrosine accompanied by a decrease in the catalytic efficiency for L-DOPA, R209H exhibited a decrease in catalytic efficiency for both L-DOPA and L-tyrosine as demonstrated by the k_{cat}/K_m values. Both of these works differ from the natural *R. solanacearum* tyrosinase (designated NP_518458) which showed a monophenolase/diphenolase activity ratio greater than one, indicating higher efficiency on L-tyrosine. This novel enzyme has an Asn (N232) at the analogous position to Arg 209 of wild-type *B. megaterium* tryosinase (Fig. 3). The authors attribute the unique activity to the pair of methionine residues attached to double HH at the CuB binding site (Fig. 3) [14]. These positions were tested in our lab by creation of a new F228M/L229M variant. The monophenolase and diphenolase activity rates of this variant were examined by HPLC and using the colorimetric assay, revealing a decrease of 30% in activity for both L-tyrosine and L-DOPA compared to wild-type (data not shown). There is a possibility that R209 could also be involved in stereospecific interaction with the carboxyl group of the substrate entering to CuB [14,20] and in the future this option will be tested by examining the kinetic parameters of tyrosine vs. tyramine and DOPA vs. dopamine.

Both the wild-type and the variant R209H were found to be stereospecific towards the L-DOPA enantiomer. However, while the K_m values of the enzymes for D-DOPA were higher than for L-DOPA, the V_{max} values of R209H were comparable for both L- and D-DOPA unlike the wild-type, in which the value for D-DOPA was lower than for the L-isomer. These findings also indicate a different orientation of the diphenol substrate in the catalytic sites of the enzymes [8]. It is also noteworthy that variant R209H and the wild-type exhibited a similar temperature stability profile (data not shown), and these results are comparable with the mouse tyrosinase and its variant Q378H [20].

In conclusion, using directed evolution we have found a new residue that influences the monophenolase/diphenolase activity ratio of tyrosinase. Furthermore our results support the hypothesis that tyrosine and L-DOPA bind differently in the active site. In addition variant R209H may be further evolved in order to obtain a biocatalyst which is efficient in production of substituted catechols due to its higher monophenolase/diphenolase activity ratio.

Acknowledgments

This research was supported by the Israel Science Foundation grant number 535/07.

References

[1] Arnold K, Bordoli L, Kopp J, Schwede T. The SWISS-MODEL Workspace: a web-based environment for protein structure homology modeling. Bioinformatics 2006;22:195–201.
[2] Bottcher D, Bornscheuer UT. High-throughput screening of activity and enantioselectivity of esterases. Nat Protoc 2006;1:2340–3.
[3] Brouk M, Derry N-L, Shainsky J, Ben-Barak Zelas Z, Boyko Y, Dabush K, et al. The influence of key residues in the tunnel entrance and the active site on activity and selectivity of toluene-4-monooxygenase. J Mol Catal B Enzyme 2010;66:72–80.
[4] Brouk M, Fishman A. Protein engineering of toluene monooxygenases for synthesis of hydroxytyrosol. Food Chem 2009;116:114–21.
[5] Claus H, Decker H. Bacterial tyrosinases. Syst Appl Microbiol 2006;29:3–14.
[6] Decker H, Tuczek F. Tyrosinase/catecholoxidase activity of hemocyanins: structural basis and molecular mechanism. Trends Biochem Sci 2000;25:392–7.

[7] Eicken C, Krebs B, Sacchettini J. Catechol oxidase—structure and activity. Curr Opin Struct Biol 1999;9:677–83.
[8] Espin JC, Garcia-Ruiz PA, Tudela J, Garcia-Canovas F. Study of stereospecificity in mushroom tyrosinase. Biochem J 1998;331(Pt. 2):547–51.
[9] Espin JC, Soler-Rivas C, Cantos E, Tomas-Barberan FA, Wichers HJ. Synthesis of the antioxidant hydroxytyrosol using tyrosinase as biocatalyst. J Agric Food Chem 2001;49:1187–93.
[10] Garcia-Borron JC, Solano F. Molecular anatomy of tyrosinase and its related proteins: beyond the histidine-bound metal catalytic center. Pigment Cell Res 2002;15:162–73.
[11] Halaouli S, Asther M, Kruus K, Guo L, Hamdi M, Sigoillot JC, et al. Characterization of a new tyrosinase from *Pycnoporus* species with high potential for food technological applications. J Appl Microbiol 2005;98:332–43.
[12] Halaouli S, Asther M, Sigoillot JC, Hamdi M, Lomascolo A. Fungal tyrosinases: new prospects in molecular characteristics, bioengineering and biotechnological applications. J Appl Microbiol 2006;100:219–32.
[13] Held M, Suske W, Schmid A, Engesser KH, Kohler HPE, Witholt B, et al. Preparative scale production of 3-substituted catechols using a novel monooxygenase from *Pseudomonas azelaica* HBP 1. J Mol Catal B Enzym 1998;5:87–93.
[14] Hernandez-Romero D, Sanchez-Amat A, Solano F. A tyrosinase with an abnormally high tyrosine hydroxylase/dopa oxidase ratio. FEBS J 2006;273:257–70.
[15] Kawamura-Konishi Y, Tsuji M, Hatana S, Asanuma M, Kakuta D, Kawano T, et al. Purification, characterization, and molecular cloning of tyrosinase from *Pholiota nameko*. Biosci Biotechnol Biochem 2007;71:1752–60.
[16] Marin-Zamora ME, Rojas-Melgarejo F, Garcia-Canovas F, Garcia-Ruiz PA. Production of *o*-diphenols by immobilized mushroom tyrosinase. J Biotechnol 2009;139:163–8.
[17] Matoba Y, Kumagai T, Yamamoto A, Yoshitsu H, Sugiyama M. Crystallographic evidence that the dinuclear copper center of tyrosinase is flexible during catalysis. J Biol Chem 2006;281:8981–90.
[18] Nolan LC, O'Connor KE. Use of *Pseudomonas mendocina*, or recombinant *Escherichia coli* cells expressing toluene-4-monooxygenase, and a cell-free tyrosinase for the synthesis of 4-fluorocatechol from fluorobenzene. Biotechnol Lett 2007;29:1045–50.
[19] Olianas A, Sanjust E, Pellegrini M, Rescigno A. Tyrosinase activity and hemocyanin in the hemolymph of slipper lobster *Scyllarides latus*. J Comp Physiol B 2005;175:405–11.
[20] Olivares C, Garcia-Borron JC, Solano F. Identification of active site residues involved in metal cofactor binding and stereospecific substrate recognition in mammalian tyrosinase. Implications to the catalytic cycle. Biochemistry 2002;41:679–86.
[21] Olivers C, Solano F. New insights into the active site structure and catalytic mechanism of tyrosinase and its related proteins. Pigment Cell Melanoma Res 2009;22:750–60.
[22] Otten LG, Quax WJ. Directed evolution: selecting today's biocatalysts. Biomol Eng 2005;22:1–9.
[23] Sanchez-Ferrer A, Rodriguez-Lopez J, Garcia-Canovas F, Garcia-Carmona F. Tyrosinase: a comprehensive review of its mechanism. Biochim Biophys Acta 1995;1247:1–11.
[24] Schweikardt T, Olivares C, Solano F, Jaenicke E, Garcia-Borron JC, Decker H. A three-dimensional model of mammalian tyrosinase active site accounting for loss of function mutations. Pigment Cell Res 2007;20:394–401.
[25] Selinheimo E, NiEidhin D, Steffensen C, Nielsen J, Lomascolo A, Halaouli S, et al. Comparison of the characteristics of fungal and plant tyrosinases. J Biotechnol 2007;130:471–80.
[26] Shuster V, Fishman A. Isolation, cloning and characterization of tyrosinase with improved activity in organic solvents from *Bacillus megaterium*. J Mol Microbiol Biotechnol 2009;17:188–200.
[27] Solano F, Garcia E, Perez D, Sanchez-Amat A. Isolation and characterization of strain MMB-1 (CECT 4803), a novel melanogenic marine bacterium. Appl Environ Microbiol 1997;63:3499–506.
[28] van Holde K, Miller K, Decker H. Hemocyanins and invertebrate evolution. J Biol Chem 2001;276:15563–6.
[29] Wang G, Aazaz A, Peng Z, Shen P. Cloning and overexpression of a tyrosinase gene *mel* from *Pseudomonas maltophila*. FEMS Microbiol Lett 2000;185:23–7.
[30] Williams GJ, Nelson AS, Berry A. Directed evolution of enzymes for biocatalysis and the life sciences. Cell Mol Life Sci 2004;61:3034–46.